

CRATER MORPHOMETRY AND SCALING IN COARSE, RUBBLE-LIKE TARGETS: INSIGHTS FROM IMPACT EXPERIMENTS. R.T. Daly¹, O.S. Barnouin¹, S.L. Light¹, M.J. Cintala², K. Hikosaka³, C.M. Ernst¹, A.A. Knuth¹, H.C.M. Susorney⁴, D.A. Crawford⁵. ¹Johns Hopkins University Applied Physics Laboratory, 11100 Johns Hopkins Road, Laurel MD, USA (terik.daly@jhuapl.edu). ²Code X13, NASA Johnson Space Center, Houston, TX, USA. ³Department of Earth and Planetary Physics, University of Tokyo. ⁴University of British Columbia, 2020 – 2207 Main Mall Vancouver, BC Canada. ⁵Crawford Technical Services, Minnesota, USA.

Introduction: Spacecraft images reveal that the asteroids Itokawa, Ryugu, and Bennu are covered with coarse, boulder-rich material [1–3]. Impactors that collide with these bodies encounter a target with extreme physical heterogeneity. Other bodies can also possess significant physical heterogeneity (e.g., megaregolith, layering, etc.). Such heterogeneities establish free surfaces and impedance contrasts that can affect shock propagation and attenuation. Therefore, such heterogeneities may also affect crater formation and excavation [4], melt generation [5–7] and crater scaling [4].

As described by [8,9], the extent to which target heterogeneity affects crater formation likely depends on how the length scale, d , of the heterogeneity (e.g., boulder size on a rubble-pile asteroid) compares to the width of the shock, w , generated by impact. Here we further test this hypothesis using impact experiments across a broad range of impact velocities and target grain sizes to systematically vary the ratio between the width of the shock and the diameter of target grains.

Methods: We carried out hypervelocity impact experiments at the NASA Ames Vertical Gun Range (AVGR) and NASA Johnson Space Center (JSC) Experimental Impact Laboratory to investigate crater formation in coarse-grained targets (Fig. 1). The experiments used alumina sphere targets (four sizes: 2, 3, 6, and 12 mm diameter). Impact speeds ranged from 1.5 – 5.5 km/s. All impacts were vertical and done under vacuum. The projectiles were also alumina spheres. Projectile diameters ranged from 1.6 to 6.4 mm. By methodically varying target grain size, projectile diameter, and impact speed, we achieved w/d ranging from ~ 0.1 to 2.

The final craters were captured using 3D scanners. The scans were processed to create 3D meshes suitable for morphometric analysis. We extracted topographic profiles across each crater at eight different azimuths and measured the rim-to-rim diameter and rim-to-floor depth of each profile. The measurements from the eight profiles were combined to compute the mean diameter, mean depth, and displaced volume for each crater. The uncertainties shown on the measurements from each crater reflect the variation observed among the eight profiles. Based on tests validating the 3D scanning system [10], this azimuthal variation dwarfs the uncertainties in the scans themselves.

Results: Figure 2 shows our results in terms of gravity-dominated π -group scaling [e.g., 11]. Although

individual spheres possess strength, the bulk target is essentially strengthless. Gravity scaling applies.



Figure 1. Photos of impact craters formed in coarse targets at the AVGR. From left to right: 2 mm, 6 mm, and 12 mm diameter alumina spheres. Crater morphology becomes increasingly irregular as target grain size increases, even for these hypervelocity impacts at ~ 5 km/s (The pre-impact surface of the 12 mm spheres was painted yellow to make the final crater more obvious.) The target bucket is ~ 60 cm across.

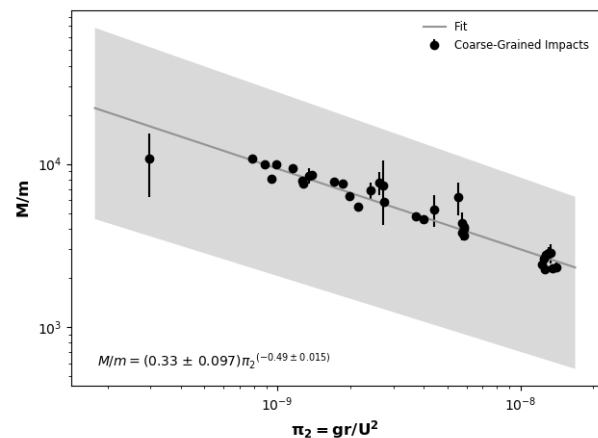


Figure 2. Cratering efficiency as a function of gravity-scaled crater size, π_2 , for all experiments in this study.

A power-law fit to the cratering efficiency data yields $\alpha = 0.49$, consistent with results for coarse sand [12] and [13–16] for #24 sand but lower than $\alpha = 0.60$ for ~ 3 mm diameter glass spheres [17]. Cratering is surprisingly efficient in these coarse targets. Over the range shown here, cratering efficiency does not vary systematically with w/d (Fig. 3). However, cratering efficiency is highly variable among experiments with similar w/d .

In contrast, impact crater depth-to-diameter ratio is sensitive to w/d . For impacts with the smallest w/d , the depth-to-diameter ratio varies widely. At $w/d \sim 0.5$, the depth-to-diameter ratio is ~ 0.2 , comparable to that of simple lunar impact craters [18]. The depth-to-diameter ratio then decreases slightly as w/d increases to 2.

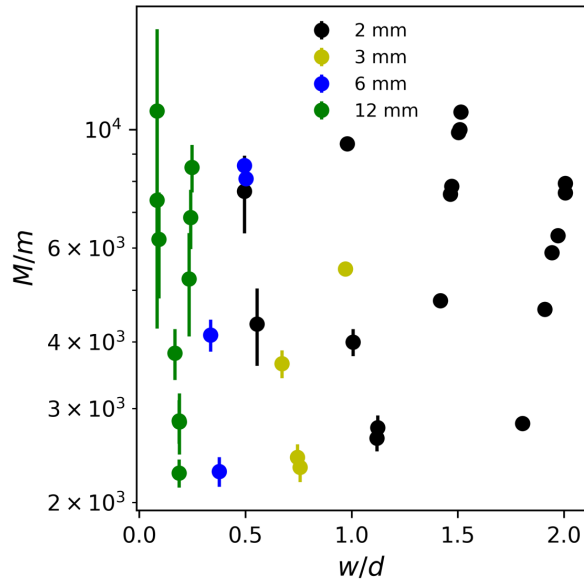


Figure 3. w/d versus cratering efficiency. Colors correspond to the diameter of the target grains; w was varied by changing impactor size and impact velocity.

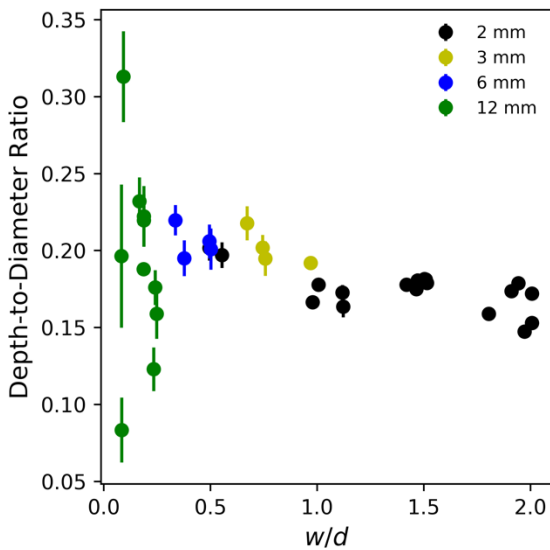


Figure 4. w/d versus depth-to-diameter ratio measured with respect to the crater rim crest. Colors correspond to the diameter of the grains in the target; w was varied by changing impactor size and impact velocity. The uncertainties on measurements from experiments with small w/d are larger because the craters are more asymmetric.

Discussion: Previous studies of impacts into coarse-grained targets have yielded mixed results. Some studies found reduced cratering efficiencies [e.g. 19], while others found that cratering efficiency was unaffected [20]. However, [20] used much higher impact speeds than [19]. Our results are more consistent with [20]. Our higher impact velocities are comparable to those in [20], but impacts at ~ 1.5 km/s were surprisingly efficient, too.

Tatsumi and Sugita [4] showed that the disruption strength of target grains is a key variable in coarse targets. According to [4], if the impact energy greatly exceeds the energy required to disrupt a target grain, cratering efficiency follows classic gravity scaling because the numerous high-velocity fragments of the grain located at the first contact efficiently transmit kinetic energy and momentum to the rest of the target [4]. We recovered multiple disrupted target grains and observed evidence for finely fragmented grains in most experiments. This observed pairing of efficient cratering with fine fragmentation is consistent with the results in [4]. Experiments at lower impact velocities will allow us to further testing this paradigm for coarse-grained impacts.

Implications: Over the range of w/d shown here, cratering efficiency is not sensitive to w/d , but the crater depth-to-diameter ratio is. Hence, crater shape may be more sensitive to w/d than crater volume, which may help to explain some of the unusual impact crater morphologies on rubble-rich Itokawa, Ryugu, and Bennu. The highly variable depth-to-diameter ratios in the coarsest targets may be due to variations in the geometry of the first contact, which may affect grain-to-grain shock propagation. Our results lend further credence to the disruption-based paradigm outlined by [4]. Therefore, an accurate interpretation of the cratering records of Itokawa, Bennu, and Ryugu requires considering the disruption strength of boulders on these bodies, as well as distribution of impact velocities on these asteroids (which has likely changed with time).

Acknowledgements: This work was supported by SSW grant NNX16AQ13G. The enthusiastic and skilled technical crews at the AVGR and JSC facilities made these experiments possible.

References: [1] Hirata et al. (2009) *Icarus*, 200, 486–502. [2] Cho et al. (2018) AGU abstract P22A-10. [3] Bierhaus et al. (2018) AGU abstract P22A-09. [4] Tatsumi and Sugita (2018) *Icarus*, 300, 227–248. [5] Cheng and Barnouin (1999) *Icarus*, 140, 34–48. [6] Kieffer (1971) *JGR*, 76, 5449–5473. [7] Wünnemann et al. (2008) *EPSL*, 269, 530–539. [8] Susorney et al. (2017) *Procedia Eng.*, 204, 421–428. [9] Susorney et al. (2018) *LPSC XLIX*, abstract 1119. [10] Light et al. (2019) *LPSC*, this meeting. [11] Holsapple (1993) *Ann. Rev. Earth Planet. Sci.*, 21, 333–373. [12] Cintala et al. (1999) *MAPS*, 34, 605–623. [13] Gault and Wedekind (1977) *Impact and explosion cratering: planetary and terrestrial implications*, 1231–1244. [14] Schmidt (1980) *Proc. LPSC XI*, 2099–2128. [15] Schultz and Gault (1985) *JGR*, 90, 3701–3732. [16] Anderson et al (2003) *JGR*, 108, 5094. [17] Barnouin et al. (in review) *Icarus*. [18] Pike (1977) *Proc. LPSC VIII*, 3427–3436. [19] Güttler et al. (2012) *Icarus*, 220, 2040–2049. [20] Holsapple and Housen (2014) *LPSC XLV* abstract 2538.